Transport by Gravity Currents in Building Fires

RONALD G. REHM, KEVIN B. McGRATTAN,
HOWARD R. BAUM and KEVIN W. CASSEL
National Institute of Standards and Technology
Gaithersburg, Maryland 20899 USA

ABSTRACT

Gravity currents (GC) are important physical phenomena which transport smoke and hot gases in corridors of buildings. In this paper, they are studied using large eddy simulations (LES). The transient Navier-Stokes (N-S) equations are numerically integrated with very high resolution, in two dimensions and with high resolution in three dimensions. The LES computations require no adjustable parameters, and are found to agree well with available experimental results in the absence of heat transfer. Fresh-water/salt-water experimental results are compared with computational results with adiabatic boundary conditions to demonstrate the validity of the model. Whereas, a high-resolution two-dimensional computation simulates very well the gravity current with adiabatic wall boundary conditions, significant wall heat transfer requires the consideration of three-dimensional effects. Heat transfer to the ceiling of a corridor from an underlying GC produces longitudinal convection rolls which significantly enhance heat losses to the ceiling and reduce the speed of progression of the GC down the corridor.

KEY WORDS: Buoyant Convection, Computational Fluid Dynamics, Fires, Fire-Induced Flows, Gravity Currents.

INTRODUCTION

When lower-density fluid is introduced at the top of an ambient fluid (or more dense fluid at the bottom of ambient fluid), the less dense fluid spreads over the ambient, forming a gravity current (GC). Gravity currents are well-known in the geophysical literature and have been studied both experimentally and theoretically for many years [1], [2]. Gravity currents are also of interest in the movement of gases in buildings. The flow of air due to heating and ventilating systems and the spread of smoke and hot gases generated by fires in buildings involve transport by gravity currents. A GC produced by a fire can transport smoke, toxic material and hot

gases, and when the building has long corridors, the current often is one of the most important mechanisms for large-scale mass and energy transport. Furthermore, the transit time for a GC in a corridor can have major impact on the egress time from the structure.

During the past several years, the authors have developed mathematical models and algorithms which describe the buoyant convection induced by a fire in an enclosure [3], [4]. The most recent advances in this model development include the capability to describe "thermally expandable" gas motion driven by "thermal elements" which evolve in complex geometries [4]. A "thermally expandable" gas is one which expands as a result of heat addition, but for which the density changes little due to pressure variations; this description is important for high temperatures induced, for example, by fires. Such a gas behaves very much as though it were incompressible, and its mathematical description has an elliptic character. The "thermal elements" are Lagrangian particles which are convected by the flow and which release heat in a prescribed fashion consistent with a mixture-fraction description of combustion. While the ability to describe thermal elements and a complex geometries are not important for the present study, the high temperature aspect of a thermally expandable gas is. With this model, it is now possible to compute the full three-dimensional structure of GCs in some detail and to compare features of GCs with experimental results. Wall or ceiling heat transfer is a critical issue for GC description, and one that has not been addressed adequately to our knowledge. Unfortunately, while detailed experimental results are available for GCs undergoing adiabatic propagation, only limited data are available when heat losses dominate the propagation [5].

In the next section, the hydrodynamic models are introduced. These models consist of the Navier-Stokes equations for a Boussinesq fluid in two dimensions and for a thermally expandable gas in three dimensions. First, adiabatic propagation of a GC is considered. We can restrict attention to only two-dimensions and to a Boussinesq fluid, where only small temperature and density variations occur. Then the model of a thermally expandable gas is presented. We report the results of a fully three-dimensional computation of a gravity current with adiabatic ceiling boundary conditions and compare it with a GC with isothermal boundary conditions. While both computations show some three-dimensional structure, the latter case exhibits essential three-dimensional behaviour in the form of longitudinal rolls which enhance heat transfer. A qualitative description of the difference between these two cases, based on past studies [1] is given, and qualitative comparison to experiments of GCs with heat transfer [5] are made. Finally, we present a summary and conclusions in Section 3.

HYDRODYNAMIC MODEL

Boussinesq Fluid

We consider the flow of a Boussinesq fluid in a rectangular enclosure, with density differences induced either by temperature or by concentration variations. To compare with experiments, we also consider the latter case; there is no difference in the dynamics between the two if proper account is taken of the sign (and size) difference between thermal expansion and density increase with salinity, as well as the differences in magnitude of the transport coefficients. Cool gas or saline water spread along the floor with exactly the same dynamics as

heated gas spreads under a ceiling, provided that there is no heat transfer (the case we examine first for comparison). Here, we compare our computations with experiments [8] [9] in which a flow is induced by the introduction of salt water into a long rectangular tank filled with fresh water. The salt water flows into the tank via a slot opening at the bottom at one end, and an equal volume of overflow is evacuated from the same sized opening at the top of the other end. For additional details on these comparisons, see [6] and [7]. Typical computed profiles of the current are shown in Figure 1.

The equations of motion for a Boussinesq fluid are

$$\mathbf{div}\,\mathbf{u} = 0$$

$$\partial(T)/\partial t + \mathbf{div}(T\mathbf{u}) = \kappa\nabla^2 T \tag{1}$$

$$\rho\,(\partial\mathbf{u}/\partial t + \mathbf{u}\cdot\nabla\mathbf{u}) + \nabla p - \rho\mathbf{g} = \rho\nu\nabla^2\mathbf{u}$$

where T is the temperature, $\mathbf{u}$ is the velocity vector, p is the pressure, g is the acceleration of gravity, ν is the kinematic viscosity, and κ is the thermal diffusivity. The latter two quantities are assumed constant. The density and the temperature are related by an isobaric equation of state $p_0 = \rho RT$ where R is the gas constant.

We employ the same scalings as used by Zukoski in his experiments [8]. All lengths are measured relative to the height of the GC h, all velocities are relative to the characteristic velocity $U = \sqrt{\beta g h}$, and time is relative to h/U. The characteristic length and velocity scales are related to the flow rate by $Q = Uh$. The total density of the mixture can be expressed as $\rho = \rho_0\,(1 + \beta\tilde{\rho})$, where $\beta = (\rho_1 - \rho_0)/\rho_0$; and ρ_0 and ρ_1 are the densities of the fresh and salt water or ambient and heated (or cooled) gas, respectively. The pressure can be written $p = p_0 + \tilde{p}$ where p_0 satisfies the hydrostatic condition $\nabla p_0 = \rho_0 \mathrm{g}$. We assume the relative density difference $\beta \ll 1$ (the Boussinesq approximation), *i.e.*, there are only small temperature differences in the heated-gas case. A prescribed flux of fluid of specified density is introduced along a segment of the bottom boundary, and, since the fluid is incompressible an equal amount of fluid must be extracted elsewhere.

The spatial grid used for the computations is uniform in each of the two directions, although the mesh length may be different in each direction. The flow variables, except for the pressure, are updated in time according to a simple second-order Runge-Kutta scheme. The pressure is determined by the solution of a system of linear algebraic equations and constitutes the bulk of the numerical computation. Other aspects of the computational scheme can be found in [7]. The resolution of the computation determines the maximum Reynolds number of the flow which can be calculated. The algorithm will fail if the Reynolds number is too large for the resolution of the grid. This feature, plus the fact that there are no adjustable parameters in the code, lead us to have confidence in the predictive capability of the computations.

Much of the large-scale structure of a GC can be described as two dimensional when heat losses are not significant. To compare the numerical simulations with the experiments quantitatively, we plot the front trajectories for both; the position of the front at each time is defined by the nose of the gravity current (the right-most point in each disturbance profile in Figure 1).

The experiment is conducted in a tank 274 cm long, 15 cm high, and 15 cm wide. Salt water is pumped into the tank through a slot 10 cm wide at a volumetric flow rate per unit length Q =17 cm^2/s, and the quantity $g\beta$ is determined to be 134 cm/s^2. Since $Q = Uh = \sqrt{g\beta h}h$, we find the height of the current h to be 1.29 cm, the ratio H/h to be 11.6, and the Reynolds number Q/ν to be 1697. For the computation, we use somewhat different conditions to reduce computational resource requirements; these compromises do not degrade the trajectory comparison however. We use a 16 × 1 rectangular enclosure (3072 × 192 cells); a ratio H/h of 8 (smaller ratios of H/h begin to show an influence of the upper boundary on the GC); the Reynolds number for the computation is 1340 in these units (somewhat less than 1697 required by the experiments); and a Schmidt number of order unity. (The Schmidt number does not affect the outcome. A computation with no mass diffusion, the infinite-Schmidt-number case, can be computed somewhat differently [6]. The trajectories computed in each case are practically indistinguishable.) Figure 2 is a comparison of the trajectories for the experiment and the simulation. The reduced tank and H/h ratios and the reduced Reynolds number from the experiments do not seem to affect the trajectories. It should be noted that flows of practical interest would have H/h ratios of order 2.

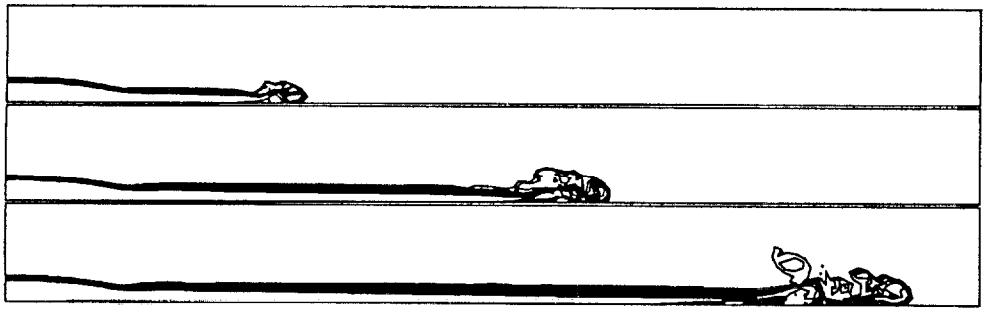

FIGURE 1: A gravity current develops as heavy fluid is pumped into the channel at the lower left. Fluid is evacuated at the upper right. The abscissa is dimensionless distance along the channel while the ordinate for each plot is heavy-fluid depth. Three times are shown during the gravity-current evolution.

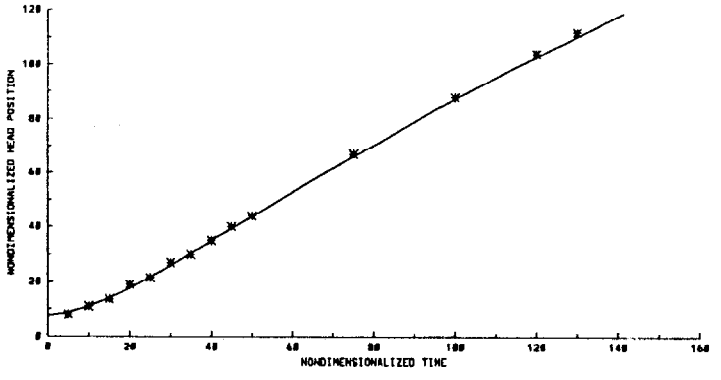

FIGURE 2: A comparison of a computed gravity current trajectory and Zukoski's experimental data (stars)

The structure of a gravity current shows a head at its leading portion where significant mixing occurs followed by laminar flow of the GC fluid [1]. As time progresses, vortices are shed regularly from the head into the ambient fluid; the beginning of this behaviour is evident in the sequence shown in Figure 1. In the study of two-dimensional boundary layer evolution induced by a vortex adjacent to a solid surface of different temperature [11], eruptions of the boundary layer have been found to occur. Such rapid eruptions of the boundary-layer fluid are known more generally to occur in unsteady boundary-layer flows. Comparison of the GC progression and these vortex-induced boundary-layer eruptions indicates that such eruptions are part of the mixing process occuring in the head of the GC.

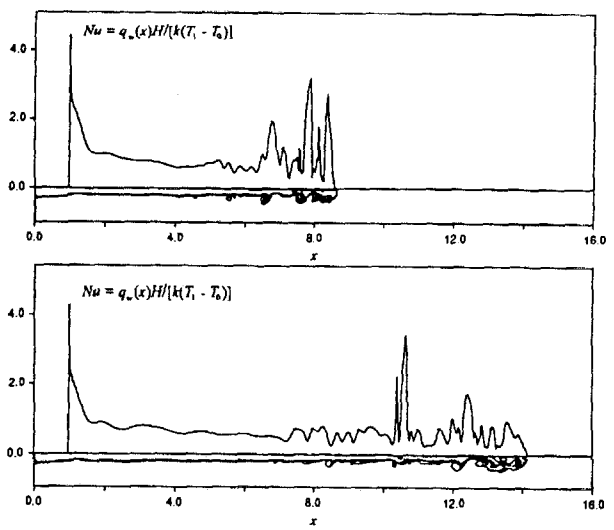

FIGURE 3: Plots of local Nusselt number $Nu = q_w(x)H/k(T_1 - T_0)$ and corresponding temperature contours at dimensionless times $t = 30$ (top) and $t = 50$. Here, x is the axial distance down the corridor from the left wall. Inflow of hot gases occurs along the top wall for a distance of one dimensionless unit in x.

Next, we consider some effects of cold-wall heat transfer (the wall remains at its initial temperature) on a GC generated by a hot layer of temperature T_1 flowing into a corridor initially at temperature T_0. Figure 3 shows temperature contours and local ceiling heat transfer coefficients as the GC progresses down the corridor. In these composite plots, the upper curve shows the Nusselt number $Nu = q_w(x)H/k(T_1 - T_0)$ at dimensionless times $t = 30$ and 50 superimposed over the corresponding temperature contours. Here q_w is the local heat flux to the ceiling and k the thermal conductivity of the gas. Note that the GC is inverted relative to those shown in Figure 1. For this computation, the parameters are the same as those for Figure 2 but with $\beta = (T_1 - T_0)/T_0$ and a Prandtl number of 0.7. (The computation required about 16 hours on an IBM RS6000 Model 58H.) The wall is assumed to remain cold providing the maximum heat transfer. Note that the heat transfer profiles are not smooth, but exhibit large variation with axial distance, particularly at the left (the inlet) and at the head of the GC. The heat transfer is very large at the inlet because the gas is the hottest there. In the head region, the mixing is greatest, causing large and intermittent heat transfer; the vortices shed by the head produce large transient heat transfer in agreement with the analysis reported by two of the

authors in another study [11].

Comparing the location of the head at each time with what was determined in the absence of heat transfer, shows that the wall heat loss slows the progression of the GC. However, this retardation of the GC is not nearly as much as would be expected by experimental results reported by Chobotov et al [5]. Furthermore, as the Reynolds number is increased with the Prandtl number fixed, the heat transfer to the ceiling decreases. These results indicate that a two-dimensional model for the GC when ceiling heat transfer are important may not be adequate. Therefore, in the next subsection we describe the fully three-dimensional model, which also must be generalized to take account of the thermal expandability of the gas.

Thermally Expandable Gas

When we consider a thermally expandable ideal gas, the equations become considerably more complicated, both mathematically and computationally. The motion of the fluid is governed by the equations suitable for low Mach number applications [3]. In addition, we assume an ideal gas, and separate the thermodynamic quantities into background and perturbation quantities as follows. The background pressure can be expressed in terms of a background temperature $T_0(t)$ and density $\rho_0(t)$

$$p_0 = R\rho_0 T_0 \tag{2}$$

These spatially averaged quantities play the same role that ambient conditions do in the Boussinesq approximation. Perturbations to each are represented by the relations

$$T = T_0(t)(1+\tilde{T}) \quad ; \quad \rho = \rho_0(t)(1+\tilde{\rho}) \tag{3}$$

and p_0 and ρ_0 are related through the adiabatic process

$$\frac{\rho_0}{\rho_\infty} = \left(\frac{p_0}{p_\infty}\right)^{1/\gamma} \tag{4}$$

The total pressure is composed of three components, the background $p_0(t)$, the hydrostatic, and a perturbation to the hydrostatic $\tilde{p}$

$$p(\mathbf{r},t) = p_0(t) - \rho_0(t)gz + \tilde{p}(\mathbf{r},t) \tag{5}$$

where z is the vertical spatial component. The equation for the mean background pressure is

$$\frac{V}{\gamma}\frac{dp_0}{dt} = \frac{\gamma-1}{\gamma}\left(\int_\Omega \dot{q}\,dV + \int_{\partial\Omega} k\nabla T\cdot d\mathbf{S}\right) - p_0\int_{\partial\Omega}\mathbf{u}\cdot d\mathbf{S} \tag{6}$$

This equation is simply a statement of conservation of volume for a thermally expandable gas. It arises by combining conservation of mass, conservation of energy and the equation of state for the ideal gas to obtain an expression for the divergence of the velocity at each

point (expressing the volume changes locally). By integrating this equation over the domain of interest, we obtain a consistency condition which determines the mean background pressure $p_0(t)$. Equation (6) shows that the background pressure is increased by the addition of heat, and decreased by the net volume outflow together with conductive heat losses at the boundaries. Usually the background quantities remain at their ambient values unless the enclosure is tightly sealed.

Here, all symbols have their usual fluid dynamical meaning: ρ is the density, $\mathbf{u}$ the velocity vector, p the pressure, $\gamma = c_p/c_v$ the ratio of specific heats, c_p the constant-pressure specific heat, T the temperature, k the thermal conductivity, t the time, $\dot{q}$ the prescribed volumetric heat release, R the gas constant equal to the difference of the specific heats $R = c_p - c_v$, and V is the volume of the enclosure.

With some manipulation [4], the equations of motion take the following form:

$$\frac{\partial \rho}{\partial t} + \nabla \cdot \rho \mathbf{u} = 0 \tag{7}$$

$$\frac{\partial \mathbf{u}}{\partial t} - \mathbf{u} \times \boldsymbol{\omega} + \nabla \mathcal{H} + \tilde{T}\mathbf{g} = \nu \left(\frac{4}{3} \nabla (\nabla \cdot \mathbf{u}) - \nabla \times \boldsymbol{\omega} \right) \tag{8}$$

$$\frac{\partial \tilde{T}}{\partial t} + \mathbf{u} \cdot \nabla \tilde{T} = (1 + \tilde{T}) \left[\nabla \cdot \mathbf{u} + \frac{1}{\gamma p_0} \frac{dp_0}{dt} \right] \tag{9}$$

The first equation is simply the conservation of mass in its usual form. The second equation is conservation of momentum, where several assumptions have been made [4] to obtain this form; see below. The third equation is the conservation of energy written for the perturbation temperature. Here, ω is the vorticity, g the gravity vector, and the ν the kinematic viscosity (assumed constant).

There has been considerable simplification of the momentum equation. The density in the pressure term has been assumed constant and equal to the ambient value. The kinetic energy term $|\mathbf{u}|^2/2$ has been combined with the perturbation pressure $\tilde{p}/\rho_0$ and written as a total pressure, $\mathcal{H}$. The replacement of the local density by its ambient value in the pressure gradient term implies that the vorticity generation induced by buoyancy is much more important than that due to baroclinic effects (*i.e.*, the non-alignment of the pressure and density gradients). This is simply a computationally convenient way of defining a buoyancy-driven flow. While the assumption breaks down at scales small enough for molecular diffusion to be an important process (as in individual flame sheets), it is an excellent approximation of the computationally resolvable length scales. For most applications, the effective kinematic viscosity coefficient ν represents dissipation on length scales below the resolution limits of the calculation. The effective Reynolds number is high enough to permit direct simulation of convective motion over a spatial range of two orders of magnitude for a three-dimensional calculation.

Simpson [1] presents a description of the anatomy of a gravity current from extensive experimental observations. He notes that there are two forms for the GC head as it progresses down a channel. First, there are billows, which are primarily two-dimensional structures. Then there

are lobes and clefs, which are essentially three-dimensional patterns; a schematic diagram illustrating this difference, taken from Simpson's book, is shown in Figure 4. We suggest that these latter patterns result from GCs which are governed by three dimensional influences such as destabilizing heat transfer arising in GCs that occur in building fires.

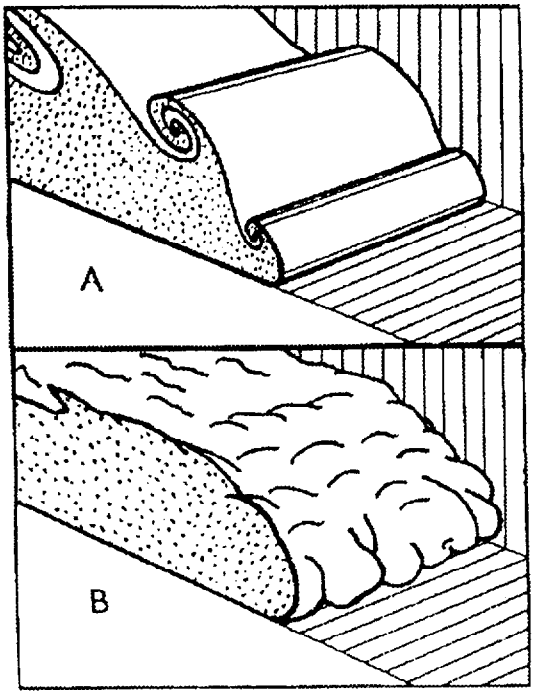

FIGURE 4: Two forms of instability at the front of a gravity current moving along the ground: (A) billows; (B) lobes and clefts. From the book of John E. Simpson, Gravity Currents, John Wiley & Sons, 1987.

Finally, Figures 5 and 6 show results from two simulations of gravity currents generated by injecting air heated to 212° C at 25 cm/s into a $6 \times 1 \times 1$ scale model corridor 0.5 meters high containing ambient air at 15° C. This is an idealization of the configuration reported in [5]. The simulations were performed using a $324 \times 64 \times 54$ grid, uniformly spaced in the horizontal directions and with variable spacing in the vertical to provide better resolution near the ceiling. In the one simulation, cold-wall (CW) boundary conditions (BCs) were used while in the other adiabatic (AD) BCs were imposed. A cold-wall BC is one for which the temperature of the wall remains constant at ambient value, 15° C in this case; this BC produces maximum heat transfer from the GC to the wall. An adiabatic BC is one for which the temperature gradient at the wall is zero; this BC produces no heat transfer from the GC gas to the wall. In Figure 5, the plots show contours of temperature along a horizontal and a vertical plane for each of the simulations described above. The upper case is for the cold-wall BCs while the lower case corresponds to adiabatic BCs.

Figure 6 shows cross-sectional plots at two axial locations, 0.33 m and 1.67 m, down the

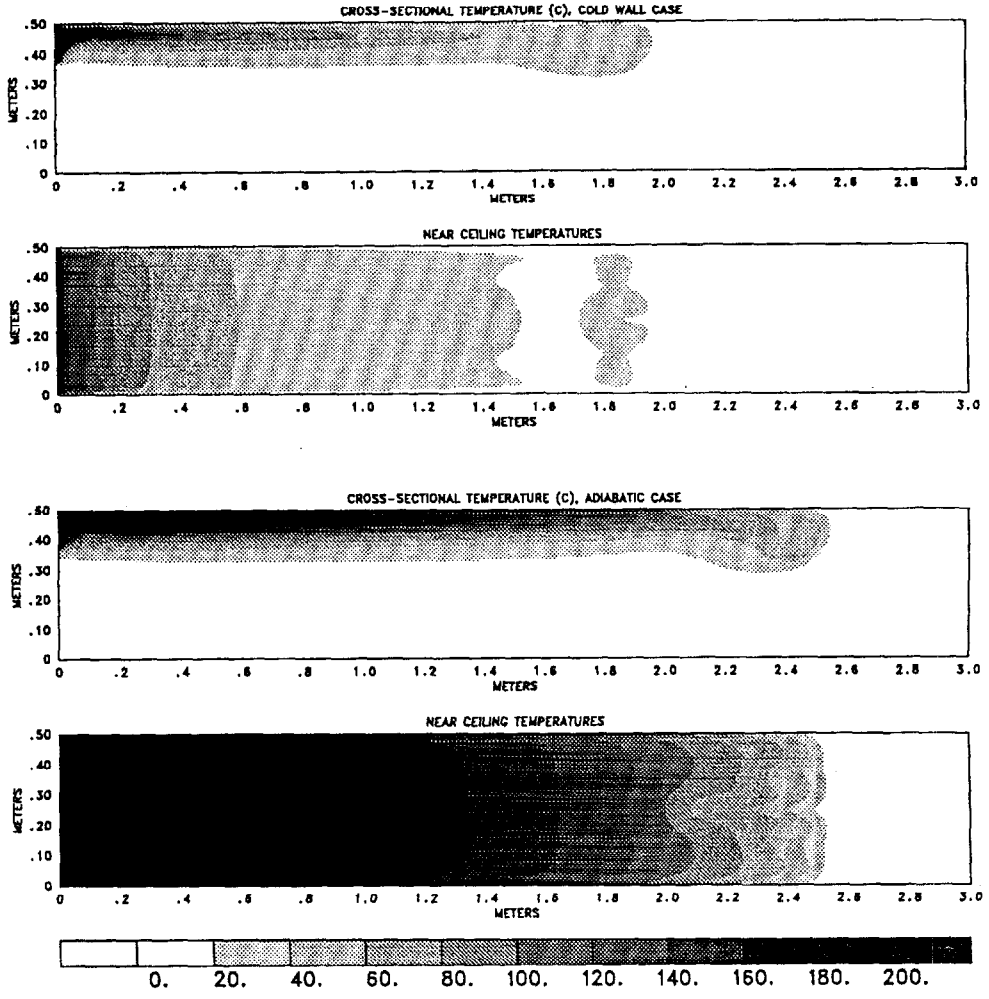

FIGURE 5: A comparison of two gravity currents, one progressing under a ceiling having cold-wall boundary conditions (top two frames) and the second having adiabatic boundary conditions (bottom two frames). The grid size for each run was $324 \times 54 \times 64$ cells, with the grid cells varying in the vertical direction so that the cells near the top of the enclosure were half a centimeter thick. The temperature of the gas exiting the vent is 212° C. The shades of the contours represent temperatures in excess of ambient (15° C).

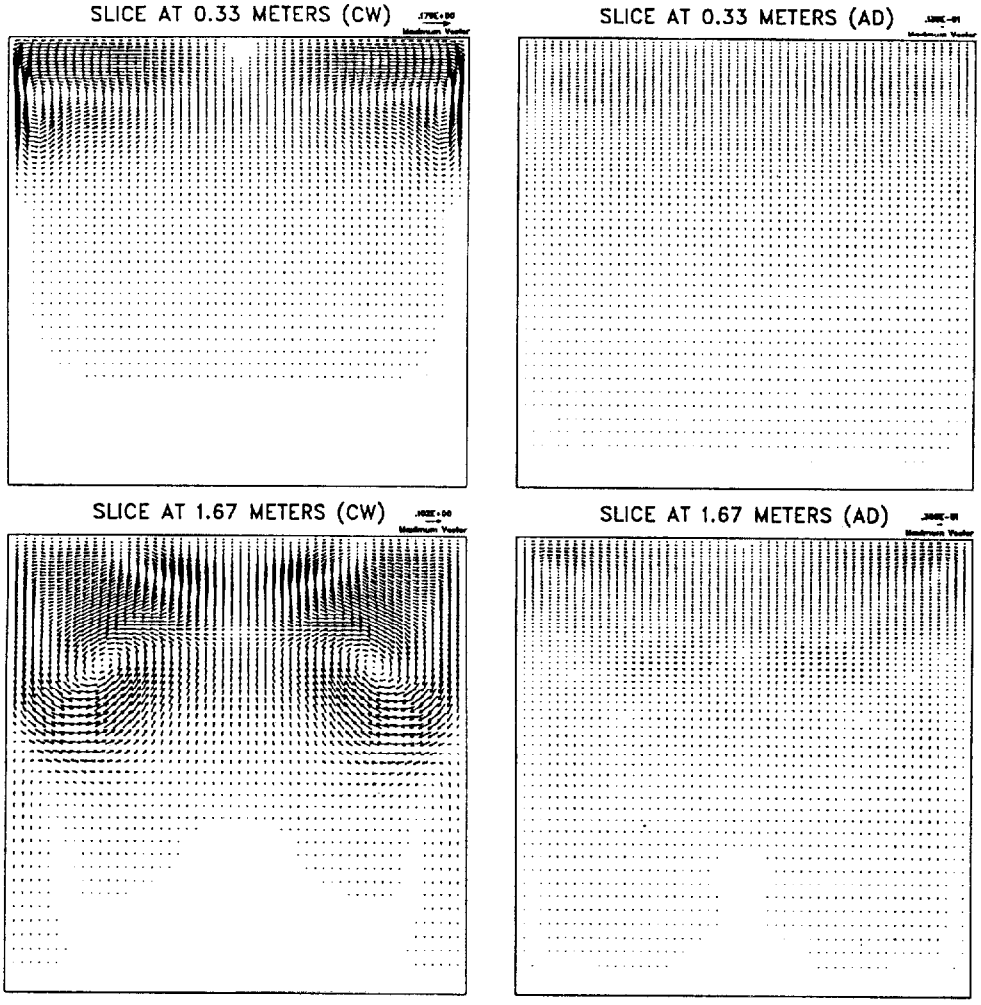

FIGURE 6: Cross-sectional plots at two axial locations, 0.33 m and 1.67 m, down the corridor for cold-wall boundary conditions (BCs) at the left and for adiabatic BCs on the right. Each plot displays the projection of the velocity vector in the cross-sectional plane.

corridor for cold-wall (CW) boundary conditions (BCs) at the left and for adiabatic (AD) BCs on the right. Each plot in Figure 6 displays the projection of the velocity vector onto the cross-sectional plane. The velocity components in all of these plots have been scaled the same so that larger velocity vectors imply greater cross-sectional circulation (axial vorticity rolls). In the plots at the left, the circulation induced by cold walls is much larger than that found in the plots of the adiabatic case on the right. Hot GC gas adjacent to the cold walls and ceiling cools by conduction to the walls. This cooler fluid is more dense (unstable) relative to the neighboring GC fluid, generating a pair of cross-sectional circulation cells as the cooled fluid sinks from the ceiling along the side walls and hot gas rises along the center-line to take its place. The intense axial vortices generated by the cold-wall BCs greatly enhance the ceiling heat transfer, rapidly reduce the temperature in the ceiling jet, and rapidly slow the GC relative to the case with adiabatic BCs (see Figure 5). These 'convective rolls' were noted explicitly in [5].

SUMMARY AND CONCLUSIONS

Gravity currents are known to be an important mechanism for smoke and hot gas transport within corridors. Wall or ceiling heat transfer is a critical issue for GC description, and one that has not been addressed adequately. With the computational fluid dynamical models available [4], it is now possible to compute the full three-dimensional structure of GCs in some detail and to compare features of GCs with experimental results. These models require no adjustable parameters and therefore have detailed predictive capability.

When heat transfer is not important, a two-dimensional, Boussinesq model adequately describes a gravity current. High Reynolds numbers, very high resolution computations have been performed using these assumptions. Boundary-layer instabilites which induce eruptions at the wall and enhance mixing in the head of the GC are captured by these computations. Cold-wall heat transfer profiles determined in this two-dimensional model show highly transient mixing and heat transfer near the head of the GC. However, the wall heat transfer is insufficient to explain the rapid temperature decrease and dramatic slowing of the GC observed in the experiments of Chobotov et al [5].

When heat transfer is important, the gravity current must be described by a fully three-dimensional thermally expandable model. Computations using this model show three-dimensional, longitudinal rolls [5] which enhance the heat transfer to the ceiling, reduce the GC velocity, and show qualitatively different behaviour for the GC propagation than in the two-dimensional case [1]. Additional detailed experimental studies of gravity current propagation when wall heat transfer is important would be very valuable.

REFERENCES

[1] J.E. Simpson, *Gravity Currents in the Environment and the Laboratory*, Halsted Press: a division of John Wiley & Sons, New York, 1987.

[2] J.S. Turner, *Buoyancy Effects in Fluids*, Cambridge University Press, Cambridge, 1973.

[3] R.G. Rehm and H.R. Baum, "The Equations of Motion for Thermally Driven, Buoyant Flows", *Journal of Research of the NBS*, Vol. 83, pp 297-308, May-June 1978.

[4] Howard R. Baum, Kevin B. McGrattan and Ronald G. Rehm, "Large Eddy Simulations of Smoke Movement in Three Dimensions," INTRERFLAM '96, Proceedings of the Seventh International Fire Science and Engineering Conference, 26-28 March 1996, St. John's College, Cambridge, England. Published by Interscience Communications, 24 Quentin Road, London, England, pp 189-198.

[5] M.V. Chobotov, E.E. Zukoski and T. Kubota, "Gravity Currents with Heat Transfer Effects," National Bureau of Standards Report, NBS-GCR-87-522, December 1986.

[6] K.B. McGrattan, R.G. Rehm and H.R. Baum, "Fire-Driven Flows in Enclosures," *Journal of Computational Physics*, Vol. 110, No. 2, pp 285-291, 1994.

[7] H.R. Baum, O.A. Ezekoye, K.B. McGrattan and R.G. Rehm, "Mathematical Modeling and Computer Simulation of Fire Phenomena," *Theoretical and Computational Fluid Dynamics*, Vol. 6, pp 125-39, Springer-Verlag, 1994.

[8] E.E. Zukoski, "Scaling Rules for Smoke Movement in Corridors", June 1990, Private communication.

[9] E.E. Zukoski, Private communication, notes and data on experiments.

[10] Chan, W.R., E.E. Zukoski and T. Kubota, "Experimental and Numerical Studies of Two-Dimensional Gravity Currents in a Horizontal Channel", Guggenheim Jet Propulsion Center Report, Cal. Tech., Pasadena, California.

[11] K.W. Cassel and R.G. Rehm, "The Unsteady Mixed-Convection Boundary Layer Induced by a Vortex," Paper submitted to The Eighth International Symposium on Transport Phenomena in Combustion, San Francisco, July 16-20, 1995.

[12] Baum, H.R. and R.G. Rehm, "Calculations of Three-Dimensional Buoyant Plumes in Enclosures", *Combustion Science and Technology*, Vol. 40, Gordon and Breach Science Publishers, pp 55-77, 1984.